Asian Journal of Chemistry Vol. 22, No. 1 (2010), 808-814

Effect of Reinforcement Volume Ratio on Thermal Conductivity of SiO_2 Reinforced Al Matrix Composite Produced by Vacuum Infiltration Method

RECEP CALIN
Department of Materials and Metallurgy Engineering, Kirikale University, Kirikkale, Turkey
E-mail: recepcalin@hotmail.com

In this study, SiO_2 powders with 105 μm particle size were filled in quartz tubes freely to form 30, 40, 50 % reinforcement volume ratios. Liquid Al7075 alloy was vacuum infiltrated into the SiO_2 compact under the same vacuum condition, the same time and at the same temperature in normal atmosphere for 3 min. After vacuuming, infiltration height and density of product composite have been determined. Microstructures of composites were investigated by SEM analysis. Two methods, finite element analysis method and experimental method, were used to determine thermal conductivity. The results of these methods were evaluated and compared. It has been found that the values of two different methods were quite near each other and thermal conductivity of composite increased with decreasing reinforcement volume ratio.

Key Words: Composites, Infiltration, SiO_2, Thermal conductivity.

INTRODUCTION

The need of materials with different properties leads development of new materials and new production techniques. Composite materials are developed in the last century and have being used in an increasing ratio. One group of these composite materials is metal matrix composites (MMCs). There are several methods for fabrication of metal matrix composites, such as casting methods, powder metallurgy techniques, *in situ* processes and infiltration methods[1-3]. Infiltration methods have also a few different application techniques[4,5]. These are pressureless (free) infiltration, pressure infiltration and vacuum infiltration techniques. Some oxides and carbides such as Al_2O_3, TiO_2, SiC and TiC, have being commonly used as reinforcement and many metals and alloys such as Al, Mg, Ti and their alloys have being used as matrix. Molten metal temperature, reinforcement powder size, reinforcement volume ratio (RVR), vacuum or pressure value, molten matrix composition, infiltration atmosphere and time are important parameters in infiltrating of molten metal into preformed reinforcement. Many studies have been made on these parameters. In infiltration processes reinforcement volume ratio of composites is important properties. Studies on particulate reinforced Al composites produced by infiltration have revealed that

reinforcement volume ratio effects infiltration behaviour and also mechanical and thermal properties in some composites[6-10]. Thermal conductivities of composite materials have recently emerged as an important subject. To measure thermal conductivity, several techniques have been developed recently. The flash technique has been widely used for determining thermal properties over wide ranges of temperatures[11,12]. In this technique which is also employed in this study, the front surface of a small sample is subjected to a very short burst of high intensity radiant energy. There are other approaches such as numerical techniques in literature[13-16] which calculate these properties, but the main change in the principle of the numerical analysis carried out in this study has been the use of real SEM images. The microstructure has also significant effect on thermal conductivity behaviour. Several studies were carried out for Si_3N_4 materials[17-21]. There is also another study that was carried out on SiAlON ceramics[22]. Thermal conductivity can be kept under control by means of micro structural modification and the attempt to correlate the microstructures with thermal conductivity behaviour play an important role[23,24]. This can be performed by modeling studies using real microstructure images. However for the application of finite element (FE), the individual intrinsic thermal conductivity values of the consisting phases are required to effective thermal conductivity (ke) calculated. In this study, the effect of reinforcement volume ratio on thermal conductivity of SiO reinforced Al composites has been investigated.

EXPERIMENTAL

Commercially pure silica (SiO_2) with 105 μm particle sizes and A7075 aluminum alloy chemical compositions are given in Tables 1 and 2 have been used as reinforcement and matrix respectively.

TABLE-1
CHEMICAL COMPOSITION OF SiO_2 USED AS REINFORCEMENT

Fe_2O_3	MgO + CaO	Al_2O_3	Na_2O	SiO_2
0.35	0.05	0.7	0.13	Balance

TABLE-2
CHEMICAL COMPOSITION OF A7075 USED AS MATRIX

Zn	Mg	Cu	Cr	Al
5.6	2.6	1.6	0.3	Balance

The instrument and the method that are given in the Calin and Citak's study[9,10] were used to produce the composite. 550 mmHg vacuum was applied to tube and tube was dipped in liquid metal in normal atmosphere. Vacuum was kept at 800 ± 5 ºC for 3 min. After 3 min vacuuming, the tubes were taken out and cooled down in normal atmosphere. Then the tubes were broken and the composites were removed from tubes. Porosity ratios of composites were determined by weighing with a

precision of 0.0001 mg. Microstructures of composites were investigated by SEM analysis.

Values of thermal conductivity of composites have been experimentally done by using the thermal diffusivity (α) value measured by an Anter brand, flashline 2000 laser flash instrument. Schematic illustration of the experimental setup is given in Fig. 1. The samples were prepared with 8 mm diameter and 3 mm height. The thermal conductivity was determined using the obtained thermal diffusion coefficient, the density and the specific heat.

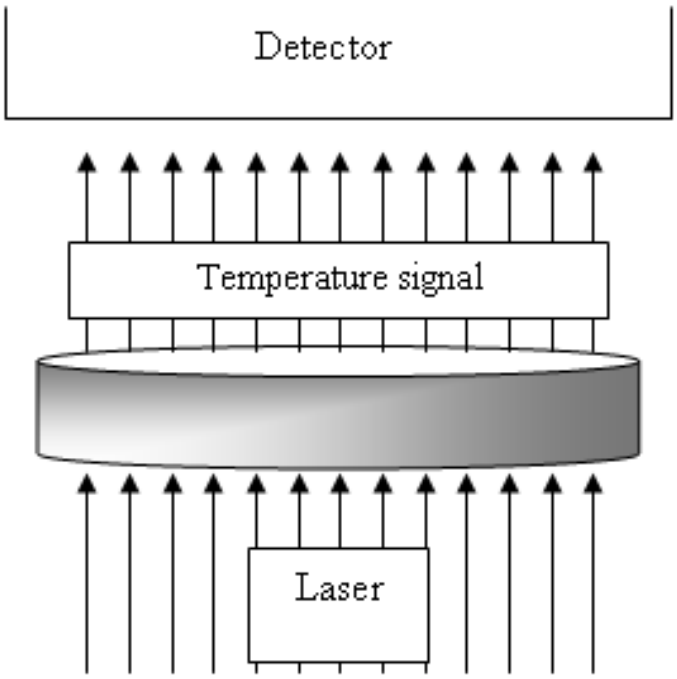

Fig. 1. Measurement of thermal diffusivity by laser flash technique

The thermal conductivity values were obtained with different analytical and numerical models and also with experimental work. The models used often are known as series (k_s), parallel (k_p), geometric mean (k_g) and Maxwell models (k_x). The basic input data in these models are the thermal conductivities and volumetric ratios of the constituent materials. These models are structurally different and depend on the type of material. The numerical model has been set up by transforming the real SEM images of the composites with 30, 40, 50 % reinforcement volume ratio. In Fig. 2, SEM micrograph of composites with 30 % reinforcement volume ratio produced by infiltration is given as a model. The numerical model has been set up

by transforming the real SEM image shown in Fig. 2b to the FE model. In Fig. 2, the area which is taken as the basis of the FE model is shown as an ellipse area.

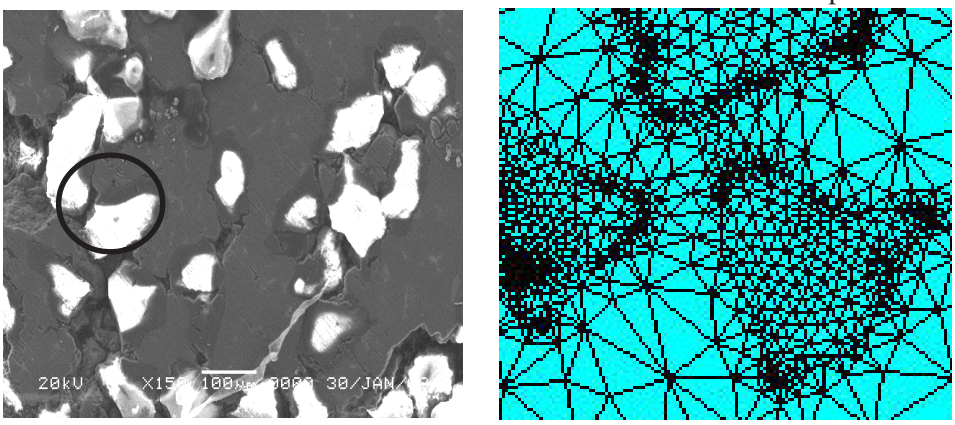

(a) (b)

Fig. 2. a) SEM micrographs of the composites with a reinforcement volume ratio of 30 % and b) a piece of the transformed numerical model

RESULTS AND DISCUSSION

The reinforcement and matrix were drawn with absolute lines by conforming to the original as much as possible. In this way, reinforcement and matrix areas are seen in grey tones in Fig. 2a have been clearly formed and the corres-ponding area ratios have been determined. These determined areas can be thought of as two different materials having separate physical properties. In this way, the problem has been reduced to a stable regime heat transfer of mixed materials having different properties as well as depending on reinforcement volume ratio. The boundary conditions are applied such that there is heat flow only in the horizontal direction and the transverse edges are assumed as adiabatic as shown in Fig. 2a) and b). Finally, the FE solution has been obtained using the usual heat transfer procedures.

Enlarged vector illustration of thermal flux between the phases from the ellipse region is given in Fig. 3. All the results of theoretical models have been employed and the results of experimental measurement are presented in Table-3.

TABLE-3
THERMAL CONDUCTIVITY VALUES (W/m?K)
OBTAINED WITH DIFFERENT MODELS

RVR	Analytic model				Numerical	Experimental
	Series (k_s)	Parallel (k_p)	Geometric mean (k_g)	Maxwell (k_x)		
30	4.236	91.930	32.655	79.792	67.460	63.210
40	3.202	78.520	20.604	65.810	39.590	36.230
50	2.574	65.650	13.000	52.934	36.190	30.520

The series and parallel models provide the lower and upper limits of the thermal conductivity, respectively. In Table-3, it can be seen that the experimental results found in this study were between these values. Maxwell that is one of analytical models gave the proximate results to experimental results. Numerical model has given very near results to the experimental results especially for composites with low reinforcement volume ratios. Table-3 also shows that both calculated and experimental thermal conductivities decreased logically with increasing reinforcement volume ratio because of high thermal resistivity of ceramic particles. Arrows in the Fig. 3 illustrate thermal flux through phases and interphases. The size and density of the arrows represent thermal conductivity and thermal flux respectively. It can be seen from Fig. 3 that the lowest thermal flux values were provided in the reinforcement. Thermal accumulation and orientation took place in the front of reinforcement colliding with a low conductivity phase from a high conductivity phase. Thermal flux increased in the matrix between two reinforcement phases because of reduction in the matrix section and heat accumulation in this section. The modeling and experimental studies showed that it is possible to set a relationship between the reinforcement volume ratio of composites and the effective thermal conductivity using SEM images of composites with different reinforcement volume ratios.

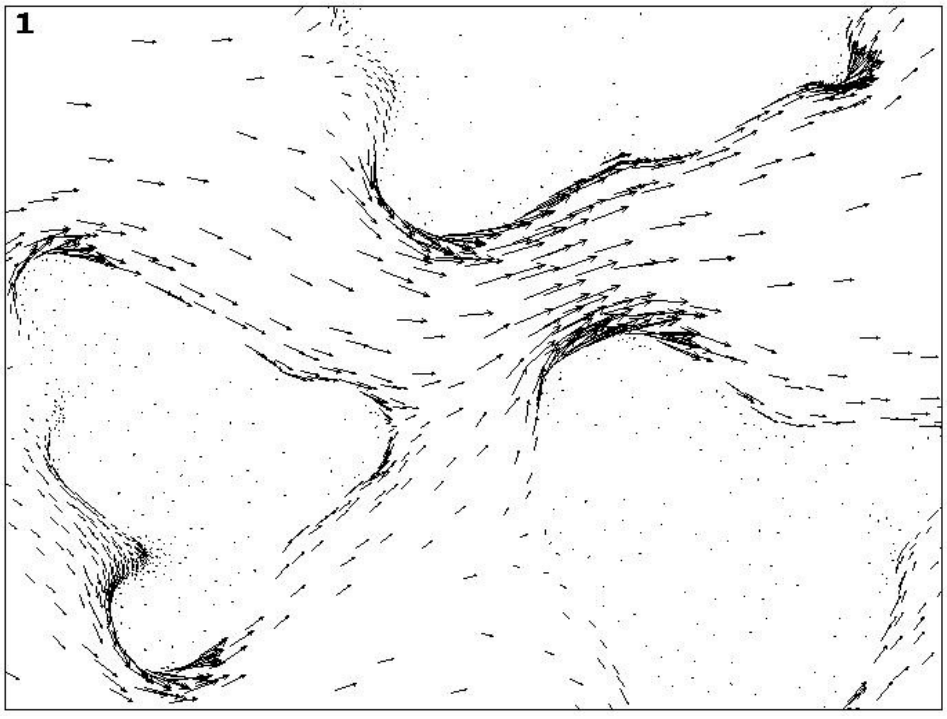

Fig. 3. Enlarged vector illustration of thermal flux in the phases of the ellipse region

Conclusion

(**1**) The effective thermal conductivity of A7075-SiO_2 composite increases with decreasing reinforcement volume ratio. (**2**) Numerical analysis provides proximate results to experimental results. Therefore numerical analysis can be used for predicting thermal conductivity of composites. (**3**) Maxwell that is one of analytical models gives the nearest thermal conductivity prediction to experimental results.

Symbols

A_m A7075 matrix surface area, m^2
A_f SiO_2 particle surface area, m^2
c Specific heat, J/(kg.K)
q" Thermal flux, W/m^2
k_e Effective thermal conductivity, W/(m.K)
k_f Effective thermal conductivity of SiO_2, W/(m.K)
k_s Thermal conductivity of series model, $\left[1/\left((1-\phi)/k_m+\phi/k_f\right)\right]$
k_g Thermal conductivity of geometric model $\left(k_m^{(1-\phi)}+k_f^{\phi}\right)$
k_m Effective thermal conductivity of A7075 matrix, W/(m.K)
k_x Thermal conductivity of Maxwell and Agari model, $\left\{k_m.\left(\frac{k_f+2k_m-2\phi.(k_f-k_m)}{k_f+2k_m-\phi.(k_f-k_m)}\right)\right\}$
k_p Thermal conductivity of parallel model, $\left\{(1-\phi)\cdot k_m+k_f^{\phi}\right\}$
R Ratios of A7075 matrix and SiO_2 thermal conductivities, k_m/k_f
ϕ Area ratios of A7075 matrix and SiO_2 Am/Af
α Thermal diffusivity, m^2/s

ACKNOWLEDGEMENT

The author gratefully acknowledged Kirikkale University for financial support (project number of 2008/55).

REFERENCES

1. D.M. Stefanescu, D.K. Dhindaw and S. Ahuja, *Metall. Mater. Trans.* **23A**, 2328 (1992).
2. W. Zhou, W. Hu and D. Zhang, **39**, 1743 (1998).
3. S.A. Gedeon and I. Tangerini, *Mat. Sci. Eng. A*, **144**, 237 (1991).
4. C.L. Buhrmaster, D.E. Clark and H.B. Smart, *J. Metals*, **40**, 44 (1988).
5. J.A. Aguilar-Martinez, M.I. Pech-Canul, M. Rodriguez-Reyes and J.L. De laPena, *Mater. Lett.*, **57**, 4332 (2003).

6. M. Elwahed and M. Asar, *J. Mat. Proc. Tech.*, **86**, 152 (1999).
7. E. Candan, H.V. Atkinson and H. Jones, *Mat. Sci. Eng.*, **35**, 4955 (1993).
8. J.J. Stephens, J.P. Lucas and F.M. Hosking, *Scr. Metal.*, **22**, 28 (1988).
9. R. Calin and R. Citak, *Mater. Sci. Forum.*, **334-356**, 797 (2007).
10. R. Calin and R. Citak, *Mater. Sci. Forum.*, **546-549**, 611 (2007).
11. S.L. Casto, E.L. Vqalovo and F. Micari, *J. Mech. Working Technol.*, **20**, 35 (1989).
12. Y. Rong, L. Jia-Jun, L. Bao-Liang, Z. Zhen-Bi and L. He-Zhuo Miao, *Wear*, **210**, 39 (1997).
13. I. Tavman, E. Girgin and R. Klavuz, Proceedings of the 9. Denizli Symposium on Composite Materials (2002).
14. R. Yang and G. Chen, *Phys. Rev. B*, **69**, 1 (2004).
15. K. Watari, K. Hirao, M. Toriyama and K. Ishizaki, *J. Am. Ceram. Soc.*, **82**, 777 (1999).
16. K. Hirao, K. Watari, M.E. Brito, M. Toriyama and S. Kanzaki, *J. Am. Ceram. Soc.*, **79**, 2485 (1996).
17. N. Hirosaki, Y. Okamoto, F. Munakata and Y. Akimune, *J. Eur. Ceram. Soc.*, **19**, 2183 (1999).
18. S.W. Lee, H.B. Chae, D.-S. Park, Y.H. Choa, K. Niihara and B.J. Hockey, *J. Mater. Sci.*, **35**, 4487 (2000).
19. H. Yokota and M. Ibukiyama, *J. Am. Ceram. Soc.*, **86**, 197 (2003).
20. N. Hirosaki, Y. Okamoto, M. Ando, F. Munakata and Y. Akimune, *J. Am. Ceram. Soc.*, **79**, 2978 (1996).
21. K. Watari, K. Hirao, M.E. Brito, M. Toriyama and K. Ishizaki, *Adv. Technol. Mater. & Mater. Process.*, **7**, 191 (2005).
22. I. Uzun, Z. Pehlivanli and B. Dogan, *Int. J. Eng. Res. Develop. Kirikkale Univ.*, **1**, 12 (2009).
23. J.S. Haggerty and A. Lightfoot, *Ceram. Eng. Sci. Proc.*, **16**, 475 (1995).
24. K. Watari, *J. Ceram. Soc. (Japan)*, **109**, 7 (2001).

(*Received*: 27 July 2009; *Accepted*: 16 September 2009) AJC-7905